NSF/RA-800053

PB81-176752

SEISMIC FRACTURE MAPPING

Prepared by:
Lewis J. Katz
Utah Geophysical, Inc.
Salt Lake City, Utah 84109

Prepared For:
National Science Foundation
1800 G Street
Washington, D.C. 20550

Under Grant: DAR-7917424

This material is based upon work supported by the National Science Foundation under award number DAR-7917424. Any opinions, finding, and conclusions or recommendations expressed in this publication are those of the author and do not necessarily reflect the views of the National Science Foundation.

SEISMIC FRACTURE MAPPING

Introduction:

On September 12, 1974 El Paso Natural Gas Company conducted a massive hydrofracture experiment at their Pinedale Unit #7 well located in Sublette County, Wyoming. Globe Universal Sciences deployed a 48 station seismic array around the well to monitor possible seismic events generated from the fracture. The array, Figure 1, consisted of four arms extending approximately one mile from the well in a north-south, east-west direction. Each station was a subarray consisting of a 24 geophone string. At the end of each string a 3-component seismometer was used. Data were recorded for approximately 12 hours prior to, during, and after the fracture. The above seismic data were given to Utah Geophysical, Inc. (UGI) for processing courtesy of El Paso Natural Gas.

In solution mining, oil and gas production, and geothermal development, the permeability of subsurface formations have to be increased to permit the flow of fluids. Usually, this is achieved by artificially fracturing the formation with either explosives or a technique known as hydrofracturing. The fractured rocks are known to generate seismic acoustical emissions. This mechanism is similar to that in which nature generates an earthquake. When an earthquake occurs, the fracture or fault is

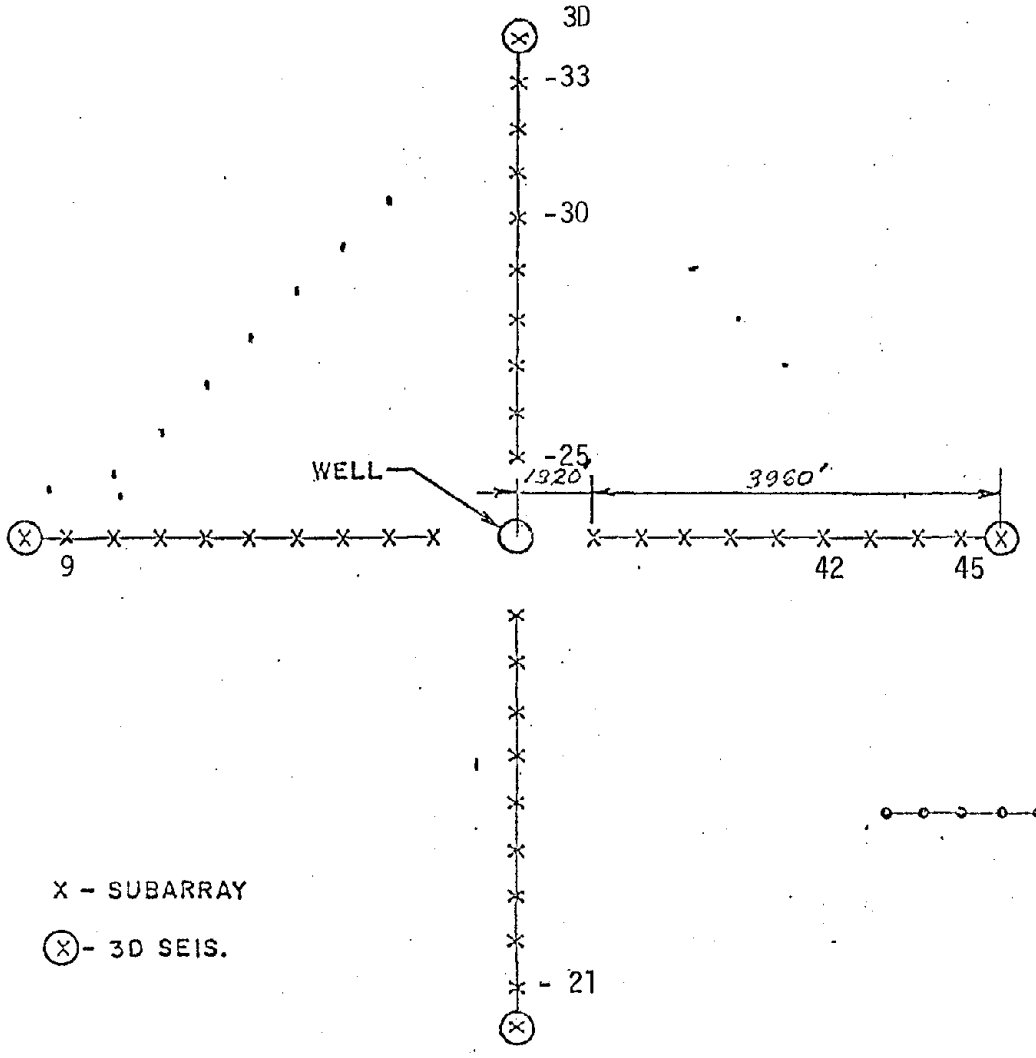

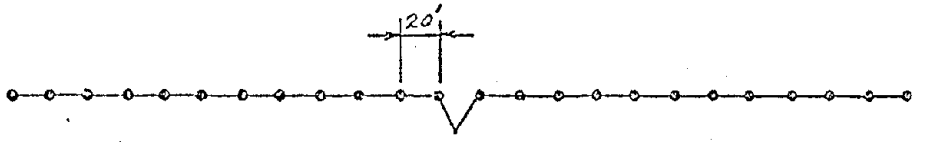

SUBARRAY OF 24 SEISMOMETERS

PRELIMINARY ARRAY DESIGN

Figure 1. Instrument deployment.

of much larger scale than that of the artificial fracture. Thus, the magnitude of the earthquake is larger and more readily observable. In hydrofracturing, the magnitude is smaller and thus the seismic events associated with the fracture are more difficult to observe. Therefore, one of the objectives of this proposal is to ascertain if these smaller seismic events can be located by using signal processing techniques. It is important to know the location of the fractures so that secondary recovery wells can be drilled to intersect these fractures and pump the fluids flowing along the fractures from the ground.

Data Processing and Analysis:

Data were delivered in demultiplexed SEG Y format. A computer program was written to transcribe these tapes to Univac 1108 format. UGI's initial objective was to use the 3-component seismometer to design a particle motion filter to separate compressional (P) waves from surface waves in the data. However, this approach had to be partially abandoned because of the quality of data. Information as to which of the three component geophones was the vertical component and which were the radial and transverse was not available. One of the three components had either very low gain or was a dead trace and there was no apparent signal beyond 80 Hz on the other components. Regardless of these problems, the first of the three component system was assumed to be the vertical component. Theoretical P-wave partical motions were calculated and compared to observed partical motions for the three component system. There was persistent agreement

of P-wave motion at 35, 40 and 70 Hz on several segments of data. Based on these findings the data would have been pre-filtered within these frequency bands to isolate the P-waves of interest. However, because of the quality of 3 component data, speculation as to the vertical component, and absence of higher frequencies it was felt that it was better to bypass this filtering step.

It is beneficial to develop an understanding of the expected magnitude, frequency, and duration of the seismic events before proceeding with processing. These properties can be estimated from the following relationships:

For magnitude (M) the relationship is:

$$L=\exp[1.43(M-4.50)] \qquad \text{(Ref. Press \& Brace, 1966)}$$

where, L is fault length in Km.

For frequency (f):

$$f=(1.97\ V_p)/(2\pi r) \qquad \text{(Ref. Brune, 1971)}$$

where, f is the corner frequency (highest expected frequency) of the P-wave spectrum.

r is the radius of the fracture if it were disk shaped.

For signal duration (S):

$$S=0.04\ \exp(0.74M) + 0.3R \qquad \text{(Ref. Esteva \& Rosenblueth, 1964)}$$

where, R is focal distance (fracture depth of 2.77Km was used).

Thus, when

L=0.0075 Km(25 ft.)	L=0.03 Km(100 ft.)
M=1.08	M=2.0
f=335 Hz	f=84 Hz
S=2.86 seconds	S=2.97 seconds

In the above example the total fracture is considered to be a series of smaller fractures migrating outward from the well bore. Amplitude attenuation with increased distance from the source also has to be taken into consideration. Seismic waves are known to attenuate at the rate of $1/R^2$ or greater. If R is taken as the fracture depth (2.77 Km.), the surface amplitude or magnitude would be 13% of those calculated. The higher frequency signals would also be attenuated much more than the lower frequencies and thus the signal duration would also appear to be less.

From the above model and considering that vehicles cause noise in a 15-30 Hz band (Long, 1971), wind noise peaks at 25 Hz (Frantti, 1963), and that 60 Hz electrical noise may be present in the data, a 61 Hz high pass filter with a 12 db/octive slope was applied to the data. Because of the large amount of data collected it was not practical to plot out all the data and visually inspect it for seismic events. Therefore, an event detector was designed. If the seismic trace had an amplitude value greater than 6 db above background level and a signal duration greater than 0.5 seconds, the computer identified it as an event and plotted the trace. Fifty possible events were located in this fashion. Two of these traces were chosen at

random for analysis.

Figure 2, shows an event located by the above event detecting method which we will refer to as event 012. As mentioned previously, a 61 Hz highpass filter was applied to the data prior to the event detection. Figure 3, shows unfiltered data for the same event. The record following this event was also analyzed and it is shown in Figures 4 (filtered) and 5 (unfiltered). Analysis of the first event of Figure 3 indicates that it has an apparent velocity of about 14,500 fps across the array and an azimuth of approach from the southwest. From signal duration and amplitude the magnitude can be estimated to be in the range of 4. Focal distance can be estimated from S-P time to be about 10,000 feet which is also the depth of the fracture. If this event was generated at depth from the fracture it would have been located within the geophone array and, thus, have an apparent velocity closer to 20,000 fps since the first arrival would be a direct wave. On the other hand, a surface blast from a seismic crew, known to be operating a few miles away, could have caused a refracted wave to be generated across the array. Examining the velocity model obtained from the Pinedale well, Table 1, the 14,500 fps refracted wave can be correlated with the 14,566 layer. Thus, this first event does not appear to be related to the fracture.

Two additional events labeled B and C follow the main event on Figure 3. Figure 5 shows an event labeled D. All of these events are attributed to some sort of electrical noise and are not seismic events. There is no move out between these events

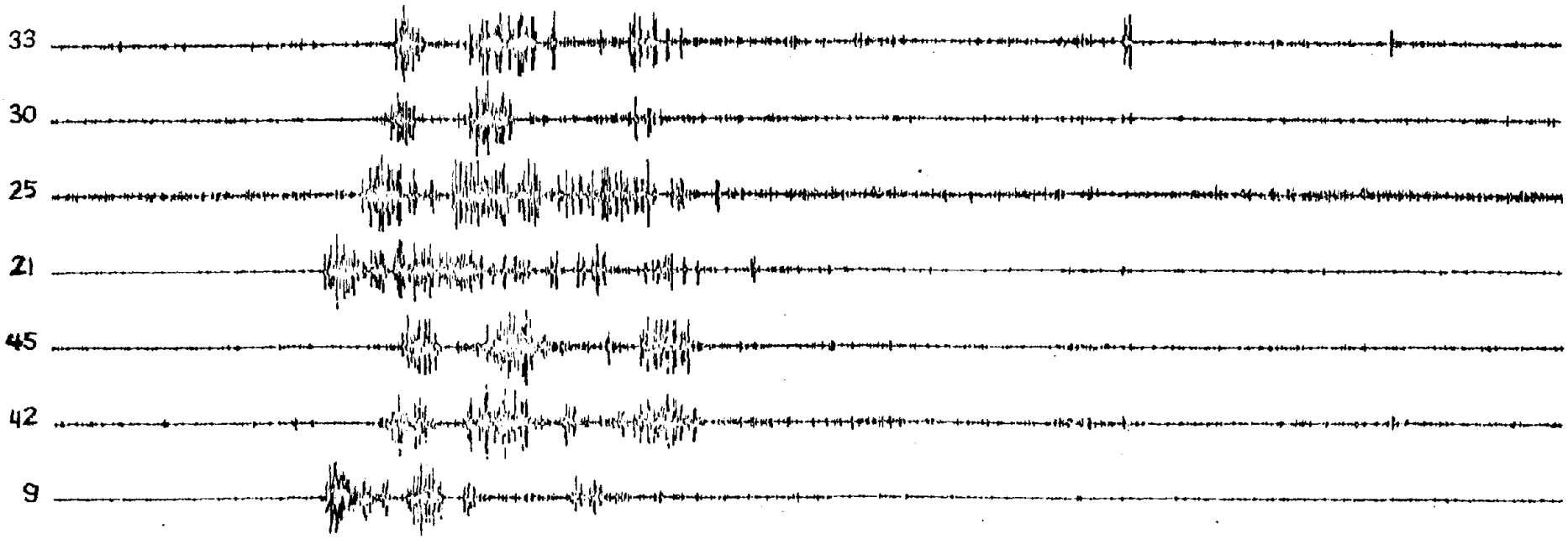

Figure 2. Event 012 (61 Hz Highpass Filtered)

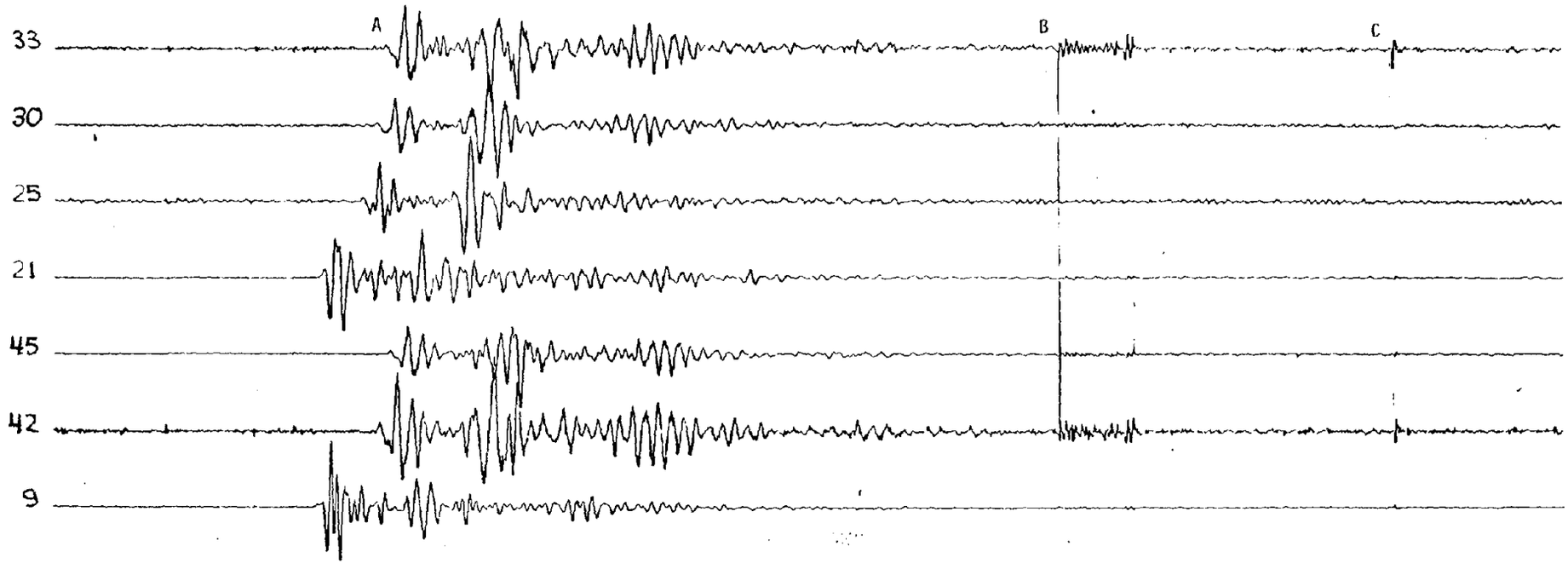

Figure 3. Event 012 (unfiltered).

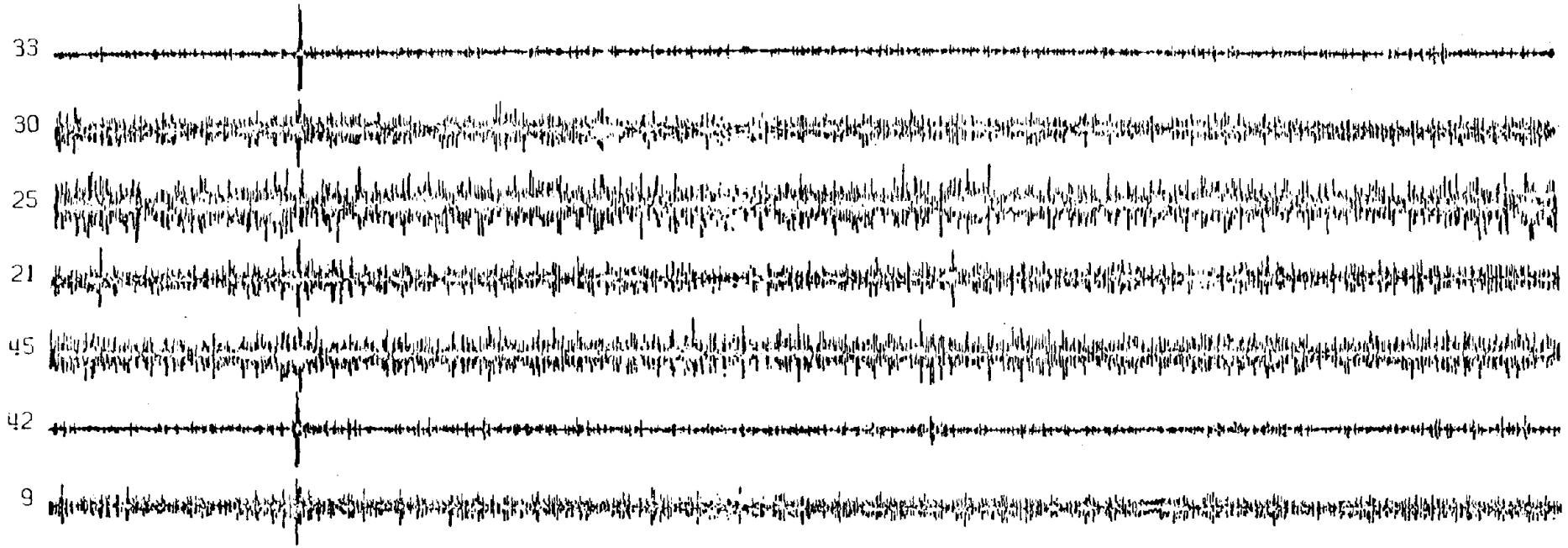

Figure 4. Event following 012 (Filtered).

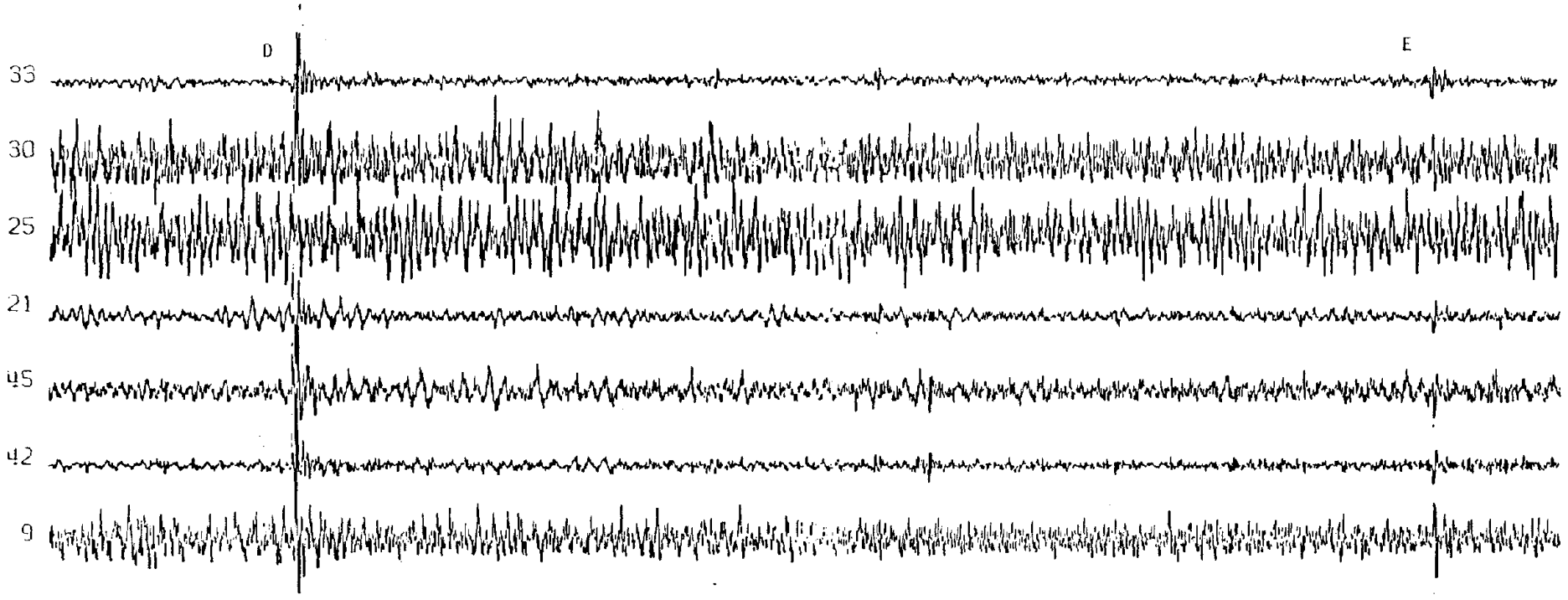

Figure 5. Event following 012(unfiltered).

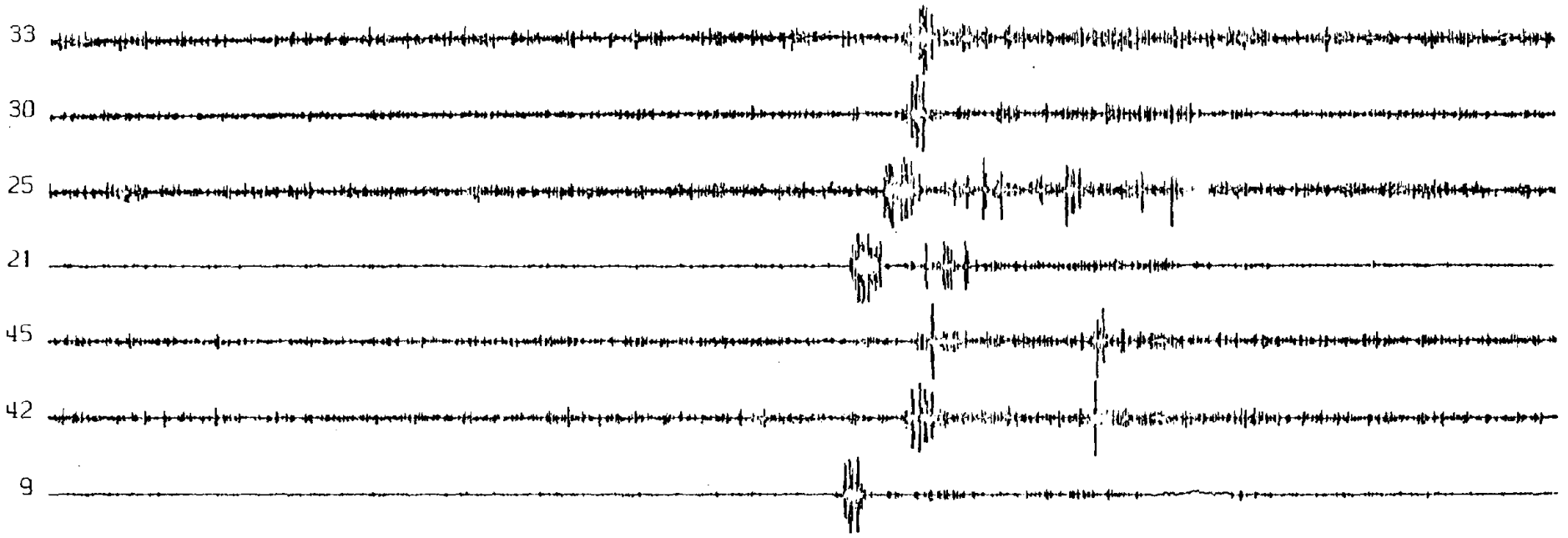

Figure 6. Event 501 (Filtered).

TABLE 1

Velocity Model
Pinedale Unit #7 Well

Depth (feet)	Velocity (fps)
0-42	3,300
42-1,000	7,000
1,000-2,000	10,373
2,000-3,000	11,025
3,000-4,500	12,275
4,500-5,700	13,857
5,700-6,775	14,566
6,775-7,710	14,724
7,710-8,220	13,673
8,220-9,250	13,054
9,250-10,250	13,423

at the various stations. That is, they all appear on all traces with the same arrival time. It is impossible for this to happen with a seismic event, except if the event were to occur several hundreds of miles below the center of the seismic array which is highly unlikely. Figure 6 shows the filtered data for an event which will be referred to as 501. Comparing this event with that appearing in Figure 2 will reveal that it has the same moveout, indicating that it too occurred outside the array possibly caused by a seismic crew. Figure 7 shows the Power Spectral Density (PSD) plot for Station 25-Tape 501.

A beam-steering multi-station array focusing technique was

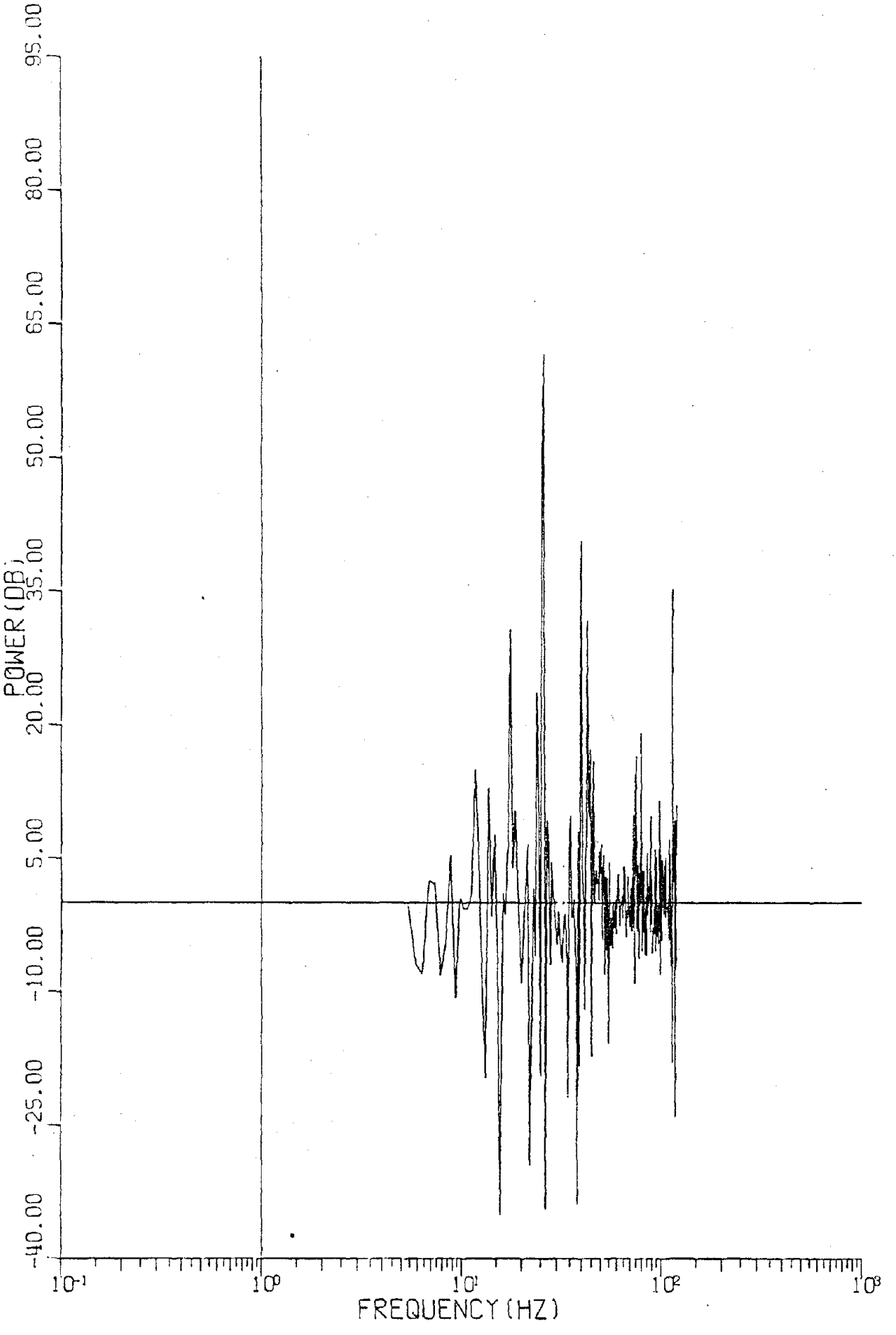

Figure 7. Power Spectral Density. STATION 25

used to process the data. A 20 X 20 array of possible noise source location points was chosen. Each of these assumed source location points were spaced at 500 foot intervals at a depth of 9100 feet. The geophone array was focused on each point by using a ray tracing algorithm to calculate travel times from each point to each geophone position. Recorded traces were then shifted by the appropriate delay times and their coherency tested. High coherency or power values occur whenever the waveforms are aligned for the proper location of the acoustic emissions generated from the fracture and lessor coherency values as one moves away from this position. Therefore, those areas showing high correlation (coherency) values on Plates 1 through 6 are indicative of the location of the fracture.

Data were correlated in 3 trace (station) segments to avoid biasing results if one of the stations were mislocated. In this manner, the results would be spatially rotated rather than decreased in value. Also, the effects of attenuation with distance to the various stations could be evaluated. Correlation results are shown on Plates 1 through 6. Tables 2 through 7 list these results. Plate 1 shows results for Stations 25, 33, 45-Tape 012 which corresponds to the data shown in Figures 1 and 3. The highest correlation value (0.1611) appears at Point 337. Referring to Table 2, at Point 337 the three traces are almost all aligned. That is, there is no moveout (Dly1=1, Dly2=0, Dly3=0). It has been shown previously that the electrical noise has zero moveout (Figure 3). In fact, what is occurring is that the electrical

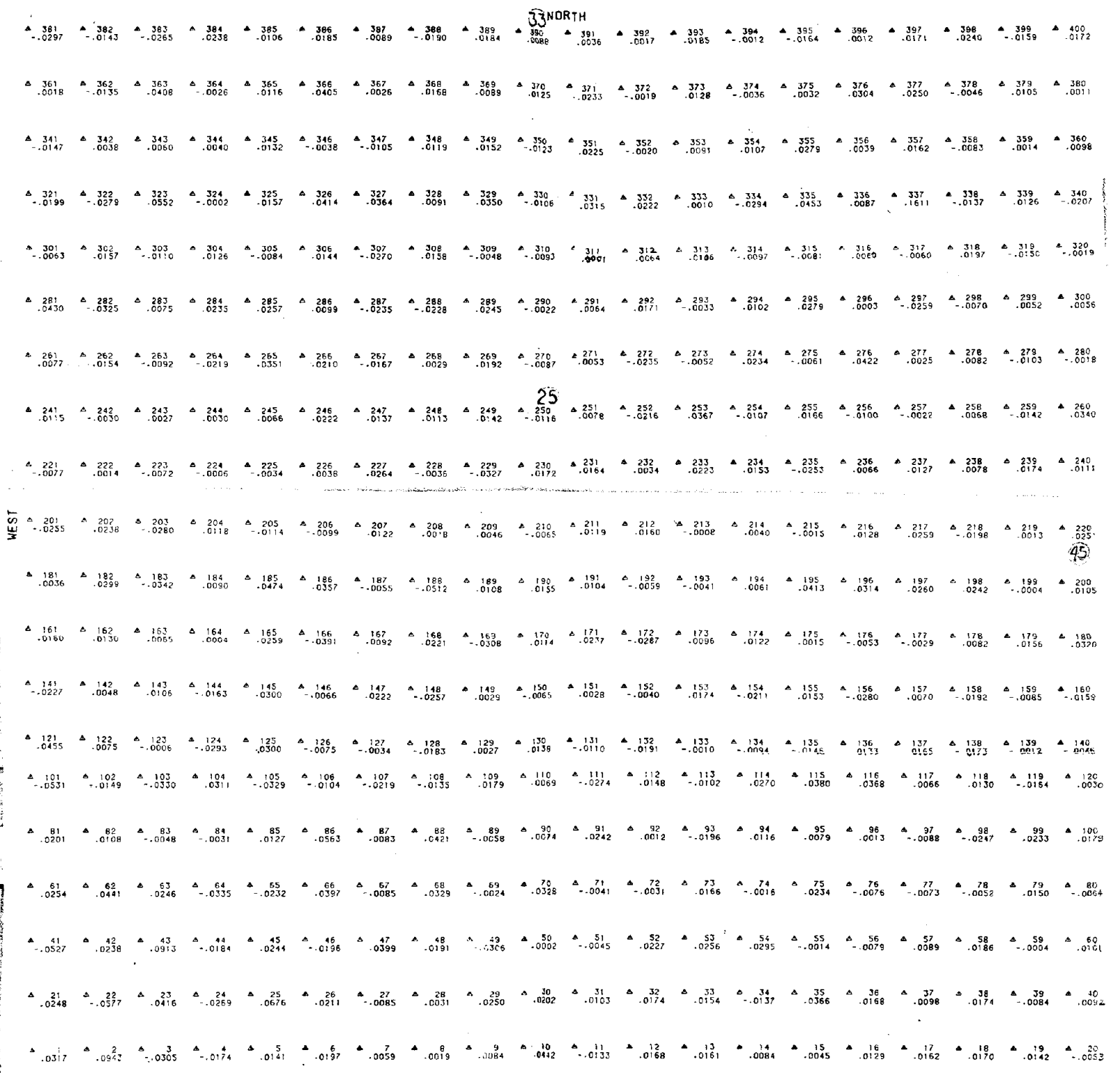

PLATE 1

LEGEND

▲ 1 .0317 CORRELATION VALUE XXXX

SCALE 1"=500'

UTAH GEOPHYSICAL. INC
SALT LAKE CITY, UTAH

SEISMIC FRACTURE MAP
STAT.25.33.45-TAPE012
PINEDALE #7 WELL

PREPARED FOR
NATIONAL SCIENCE FND.

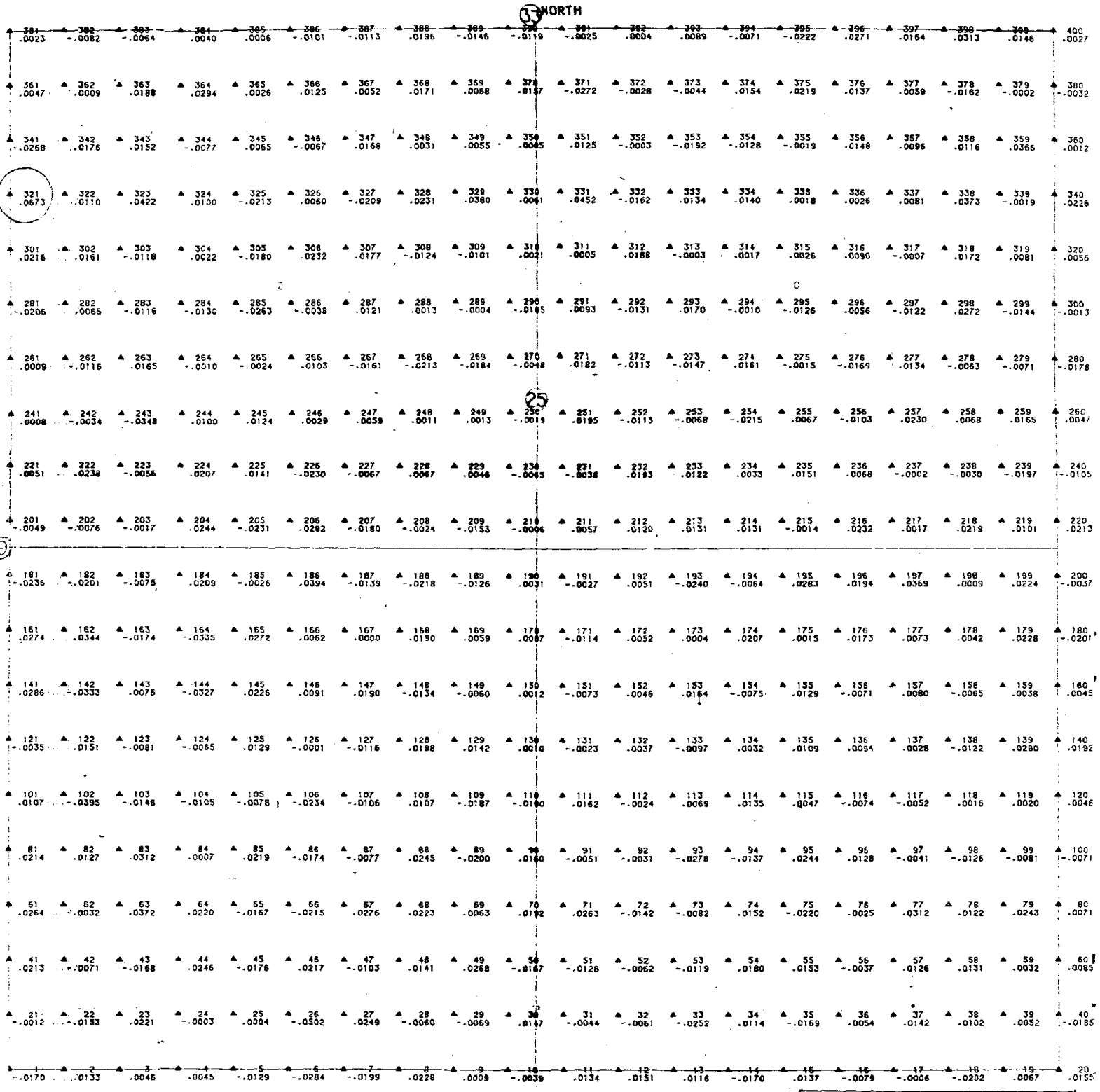

UTAH GEOPHYSICAL, INC
SALT LAKE CITY, UTAH

SEISMIC FRACTURE MAP
STAT.25,33,9-TAPE 012
PINEDALE #7 WELL

PREPARED FOR
NATIONAL SCIENCE FND.

LEGEND

▲ -.0170 CORRELATION VALUE
XXXX

SCALE 1"=500'

PLATE 2

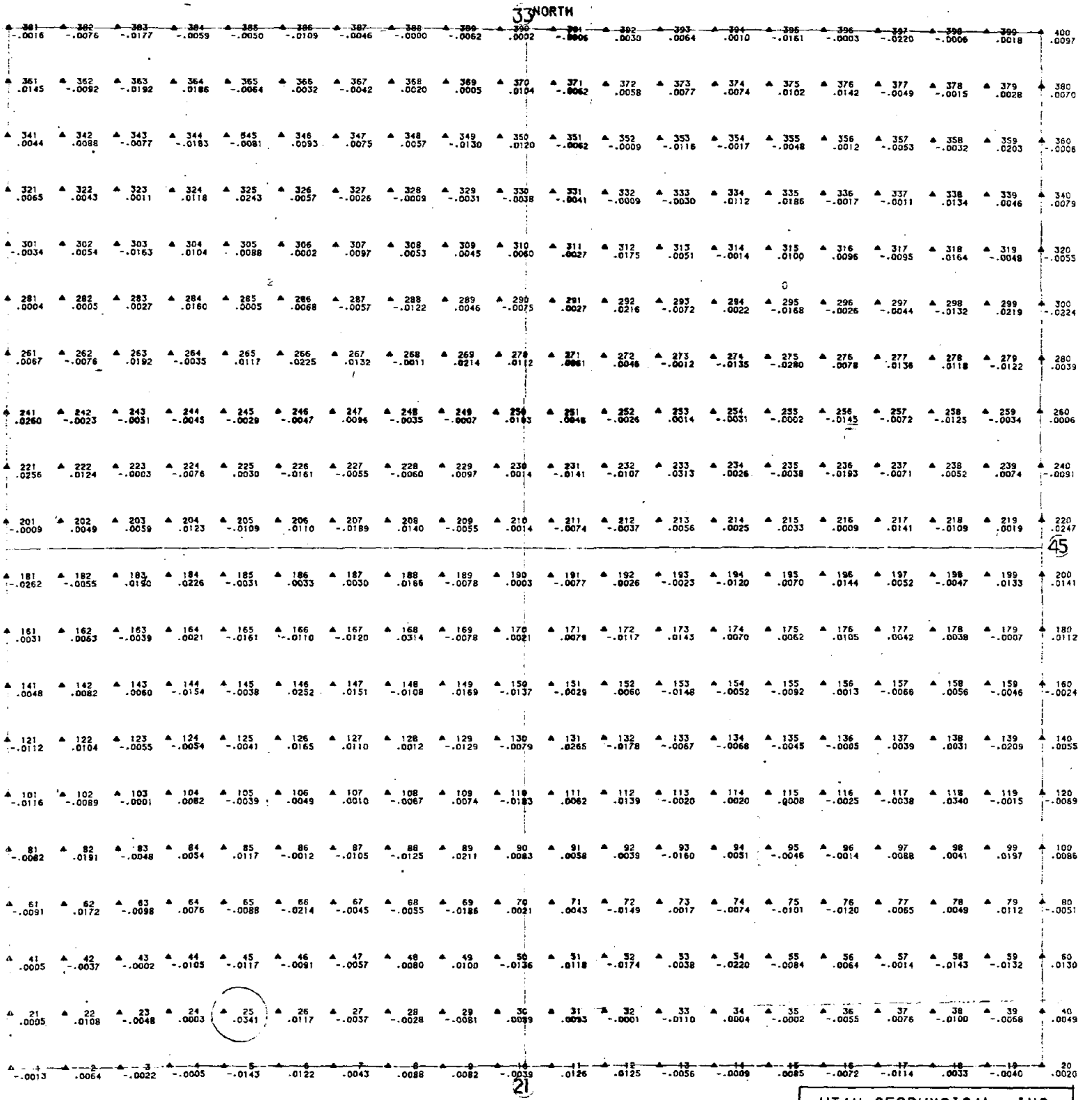

Reproduced from best available copy.

LEGEND

-.0013 CORRELATION VALUE XXXXX

SCALE 1" = 500'

UTAH GEOPHYSICAL, INC
SALT LAKE CITY, UTAH

SEISMIC FRACTURE MAP
STAT.21,33,45-TAPE012
PINEDALE #7 WELL

PREPARED FOR
NATIONAL SCIENCE FND.

PLATE 3

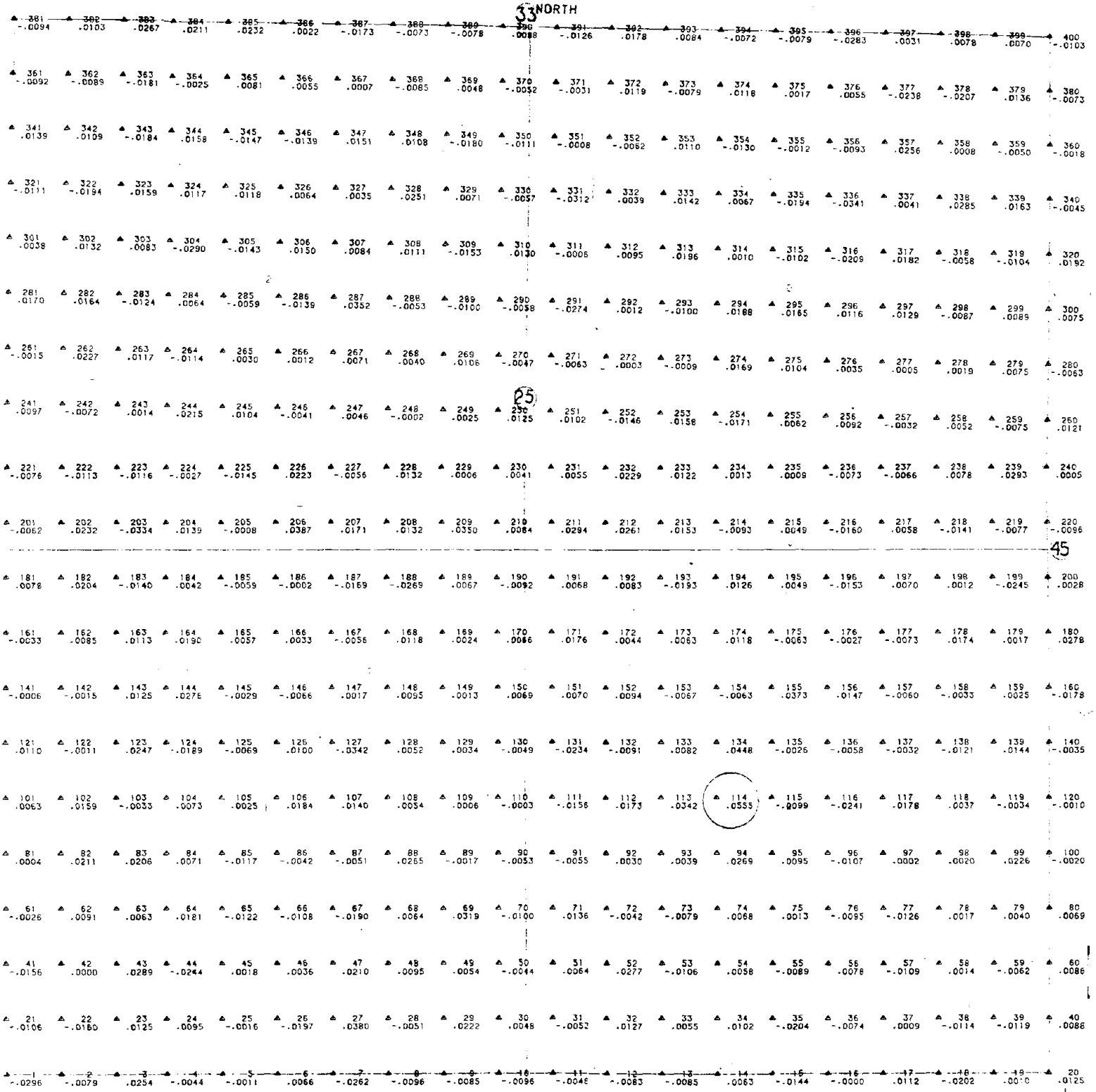

UTAH GEOPHYSICAL, INC SALT LAKE CITY, UTAH	
SEISMIC FRACTURE MAP STAT.25,33,45-TAPE 501 PINEDALE #7 WELL	
PREPARED FOR NATIONAL SCIENCE FOUNDAT	

LEGEND

CORRELATION VALUE
XXXX

SCALE 1"=500'

PLATE 4

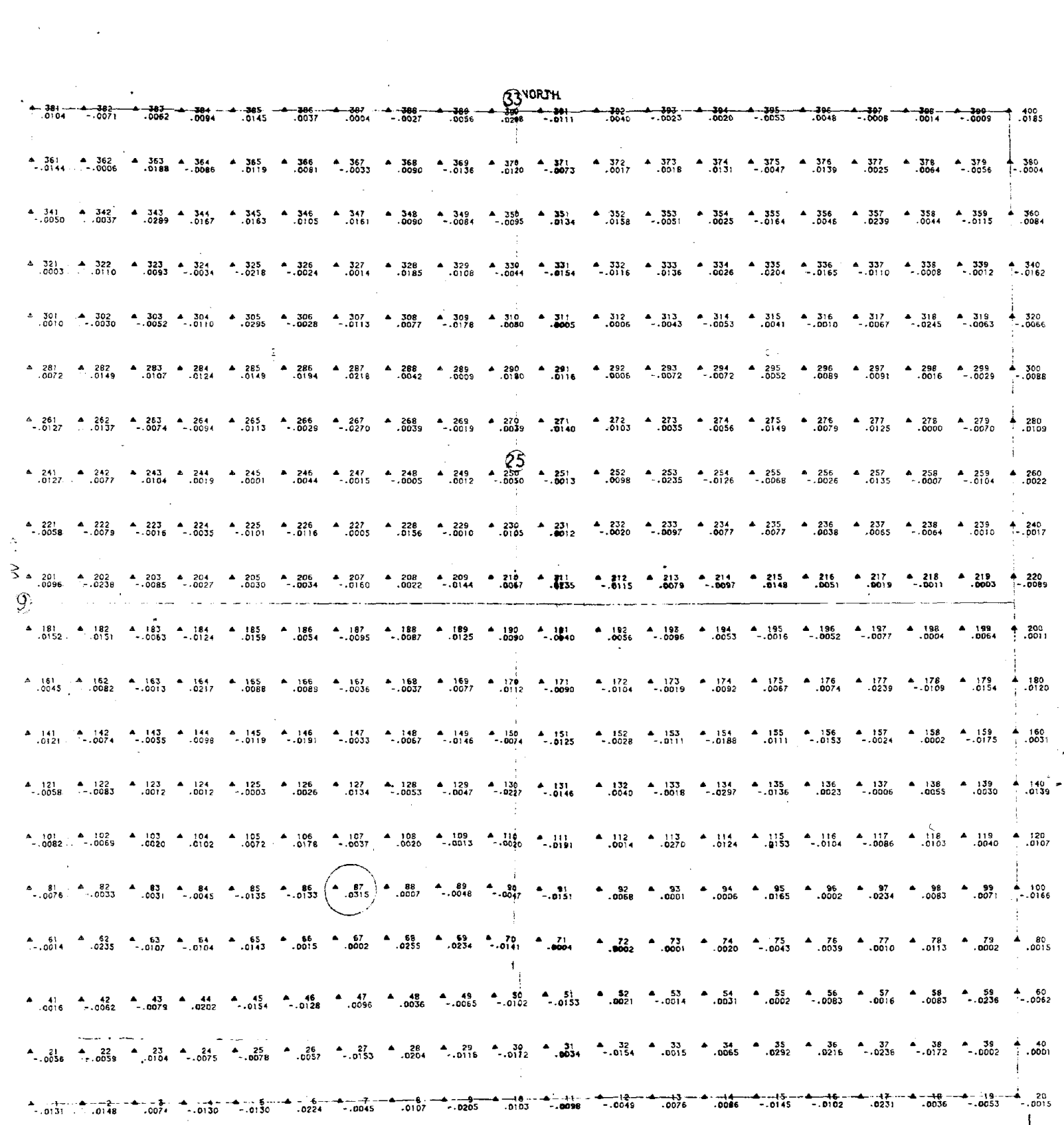

LEGEND

1 -.0131 CORRELATION VALUE XXXX

SCALE 1" = 500'

UTAH GEOPHYSICAL, INC
SALT LAKE CITY, UTAH

SEISMIC FRACTURE MAP
STAT.25.33.9-TAPE501
PINEDALE #7 WELL

PREPARED FOR
NATIONAL SCIENCE FND.

PLATE 5

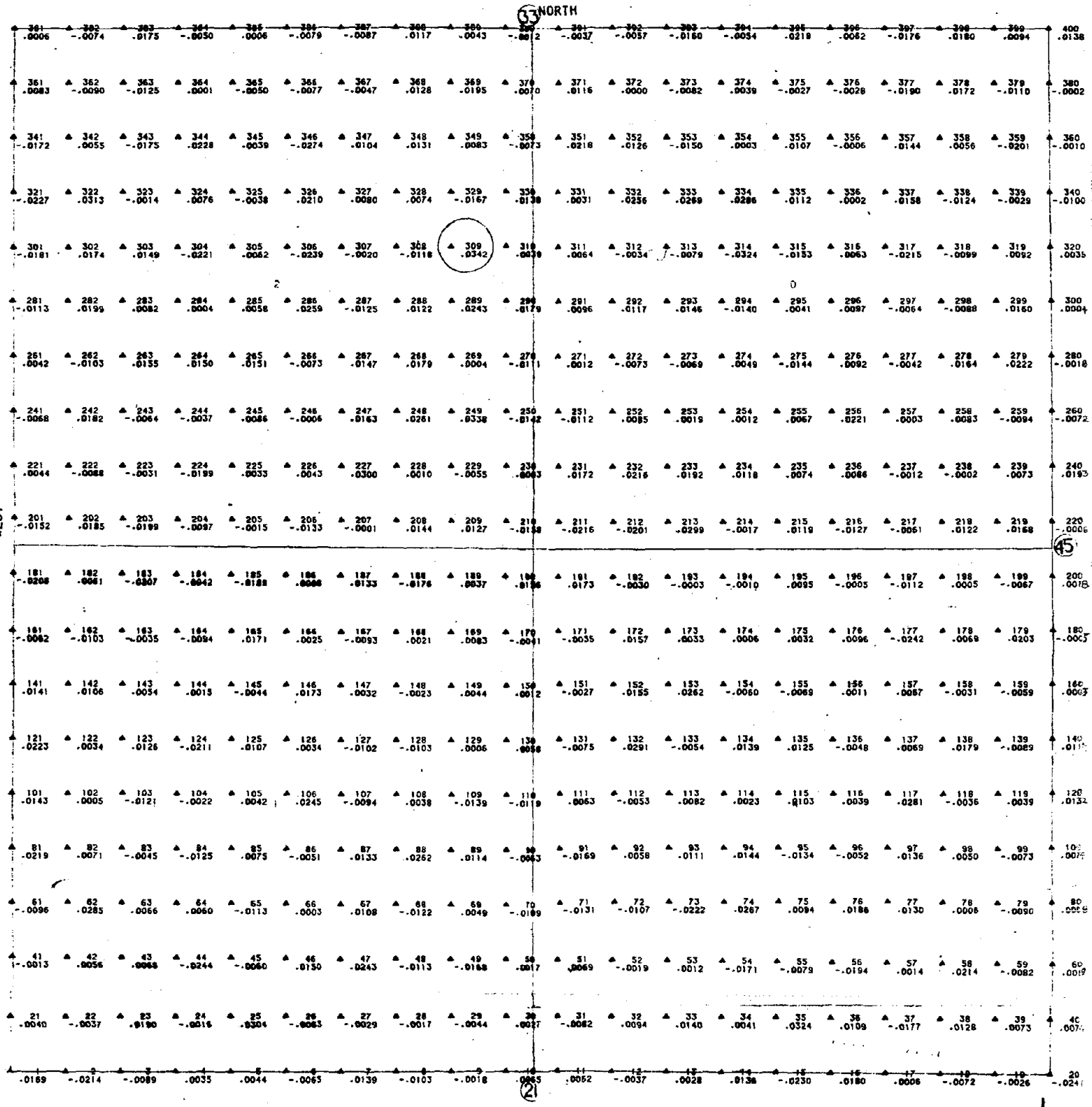

Reproduced from best available copy.

LEGEND

▲ .0169 LOCATION NUMBER
CORRELATION VALUE

SCALE 1"=500'

UTAH GEOPHYSICAL, INC
SALT LAKE CITY, UTAH

SEISMIC FRACTURE MAP
STAT.21,33,45 - TAPE 50
PINEDALE #7 WELL

PREPARED FOR
NATIONAL SCIENCE FND.

PLATE 6

noise is in phase for this position causing the high correlation value. It is interesting to take note of the power and effectiveness of the beam-steering approach used in this study. Even with a large event present (see Figure 3), the beam-steering technique locks in on smaller magnitude events that the array focuses on. The electrical noise is obviously going to bias any results occurring with the data set of Tape 012 (Plates 1 through 3). However, a high correlation value at Point 25 on Plates 1 and 3 should be noted. The traces involved do not have zero moveout for this position (see Tables 2 and 4). If the results from the data set of Tape 012 were to be composited, Point 25 would have a maximum correlation value.

Analyzing the data set of Tape 501 (Plates 4 through 6), Point 337 for Stations 25, 33, 45 (Plate 4), at which position the traces would have approximately zero moveout (Table 5), there is a very small correlation value. This establishes the fact that there is no electrical noise present in this data as was in the case of the previous Tape 012. Stations 25, 33 and 45 (Plate 4) show a high correlation value at Point 114. Stations 25, 33 and 9 (Plates 5) show a maximum correlation value at Point 87. Point 87 is aligned with Point 25 which was previously discussed as having a maximum composite correlation value on Tape 012. Data on Tape 012 were collected after data on Tape 501. Therefore, it can be hypothesized that the fracture has migrated from Point 87 to Point 25. It should also be noted that on Plate 5 there is a high correlation value near Point 114 (actually Point 113) which

would agree with results of Plate 4.

Conclusions and Interpretation:

In general, the correlation values were low. This can be accounted for by the fact that a seismic event generated from the fracture is going to be quite small to start with and a further reduction in size can be expected from attenuation with focal distance before it arrives at the seismometers. Another problem that probably occurred at this site is that some of the seismic energy was reflected back into the ground. The velocity profile of Table 1 shows a 14,724 fps high velocity layer overlying a lower velocity layer in which the fracture occurred (at 9100 ft.). The high velocity layer would have the effect of reflecting seismic energy back into the earth. Regardless of these problems, and those of having cultural and electrical noise in the data, it appears that a southwest striking fracture (Points 87 and 25) could be mapped. Evidence of this fracture extending in a northeasternly direction could not be substantiated since electrical noise in the data forced the correlation in this direction. The existance of a southeasternly fracture is also possible (Point 114). Additional processing of this data would be needed to increase confidence in and confirm these finding. This same survey at a shallower depth, in the absence of a high velocity layer and electrical noise could be expected to have positive results. In conclusion, we have found fracture mapping using a seismic beam-steering method feasible, although, results from the data set used in this study have not been confirmed.

Pages 17-64 have been removed.

Due to legibility problems, the following has been omitted:
Table 2 through Table 7*

*These pages are available upon written request from:
Mr. Lewis J. Katz
P.O. Box 9344
Salt Lake City, UT 84109

REFERENCES

Brune, J. N. (1971). Tectonic stress and the spectra of seismic shear waves from earthquakes, J. Geophys. Res., 76, p. 5002.

Esteva, L. and Rosenblueth, E. (1964). Espectros de templores a distancias moderaradas y grandes, BSMIS, Mexico, 2, p. 1-18.

Frantti, G. E. (1963). The nature of high frequency earthnoise spectra, Geophysics, V. 28, No. 40, p. 547-562.

Long, L. T. (1971). Investigations of seismic road noise, Engineering Experimental Station, Georgia Instit. Tech., Rept. A-1357.

Press, F. and Brace, W. F. (1966). Earthquake prediction, Science, 3729, p. 1575-1584.